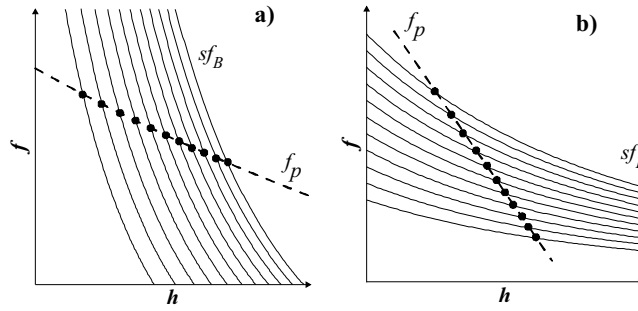


**Figure 1.** Dynamic spectrum of the solar burst "fingerprint" at the decameter wavelengths 22.07.2004. The rectangle selects a spectrum fragment with the most distinctively resolved spectral stripes, which is chosen for the numerical analysis. The dotted lines give schematically the form of the fine structure lines.

the increase in the frequency resolution resulted in detection of the fine spectral details, the analysis of which makes it possible to get information about the physical conditions and the processes in the upper corona.

In the present paper a fine structure in the dynamic spectra observed on 22.07.2004 against the background of the type IV continuum in the frequency range 20-30 MHz for one and a half minute (Melnik *et al.*, 2008) is discussed. In 2004, the solar radio emission was observed by only three sections of the UTR-2 radio telescope with effective area 30000 m<sup>2</sup> and antenna pattern size 1° × 13°. The signal was recorded by a 60-channel spectrometer with a frequency band of 3 KHz for each channel. The frequency spacing between the channels was 340 KHz, so the entire working frequency band from 10 to 30 MHz was overlapped. The location of the channels was chosen so as to eliminate interference. To visualize the dynamic spectrum, the gaps between the channels were supplemented by the values of the neighboring channels. A 60-channel spectrometer provided a time resolution of 10 ms (but in 2004 the observations were performed with 100 ms resolution) and a sensitivity of 10<sup>-23</sup> W/m<sup>2</sup> Hz.

The dynamic spectrum of the burst under discussion shown in Figure 1, looks like a fingerprint, and following Melnik *et al.*, 2008 it is this denotation which will be used subsequently. The fine structure as a system of quasi-harmonic stripes parallel drifting in time, or the so-called zebra pattern (ZP), is often observed in the solar dynamic spectra at the meter and decimeter wavelengths (see, for example, Aurass *et al.*, 2003, Chen *et al.*, 2011, as well as reviews by Chernov, 2006, Zlotnik, 2009). However, at first sight the burst under discussion can hardly be attributed to ZP. Rather, here exist not the stripes of enhanced radiation equally spaced in frequency, but quasi-periodic bursts of enhanced radiation, that is a fine temporal, rather than frequency, structure. Thus, it seems quite different to consider it as a typical ZP and explain it by the double



**Figure 2.** Model of a typical ZP source in the meter-decimeter wave band: dependence of the electron number density and the harmonics of the electron cyclotron frequency on the coordinate along the nonuniform source. Two panels refer to the cases where the magnetic field changes with the height faster (a) and slower (b) than the electron number density.

plasma resonance (DPR) effect in a coronal trap. Nonetheless, as will be shown below "the fingerprint" is easily explained in the framework based on the DPR effect, and it really represents some kind of the usual ZP.

## 2. DPR effect in the solar corona

We recall in a nutshell the DPR effect in the corona (Zlotnik, 2009; Zheleznyakov and Zlotnik, 1975; Kuijpers, 1975; Winglee and Dulk, 1986; Kuznetsov and Tsap, 2007; Zlotnik and Sher, 2009; Zheleznyakov, 2000). It is assumed that a magnetic flux tube is filled with an equilibrium weakly anisotropic plasma with electron number density  $N$  as well as a small amount of the electrons with electron number density  $N_e$  and the non-equilibrium distribution over the velocities perpendicular to the magnetic field:

$$N_e \ll N. \quad (1)$$

Then at the discrete levels where the frequency of the upper hybrid resonance  $f_{UH} = (f_p^2 + f_B^2)^{1/2} \approx f_p$  (the last approximate equality is valid under the condition of weak anisotropy  $f_B \ll f_p$ ) coincides with harmonics of the electron cyclotron frequency  $f_B$ , i.e.

$$f_p = sf_B, \quad (2)$$

enhanced generation of the plasma waves propagating perpendicular to the magnetic field takes place. In the above relations  $f_p = (e^2 N / \pi m)^{1/2}$  is the plasma frequency,  $f_B = eB / mc$  is the electron cyclotron frequency,  $B$  is the magnetic field,  $e$  and  $m$  are the electron charge and mass,  $c$  is the light velocity, and  $s$  is the harmonic number.

Figure 2 shows the model of the ZP source illustrating the DPR effect: it is the dependence of the plasma frequency and harmonics of the electron cyclotron frequency on the coordinate along the flux tube at a given time. For simplicity, here and everywhere below we suppose that the nonuniform source is elongated

vertically in the corona, so the coordinate along the source is the height  $h$  above the photosphere. Evidently, the DPR effect is realized only at different gradients of the magnetic field and electron number density. Radiation stripes arise at the levels corresponding to the points of intersection of these curves. The frequency spacing between stripes is determined by the electron cyclotron frequency and the ratio of the gradients of the magnetic field and the electron number density. If the magnetic field changes with the height faster than the electron number density, then the frequency spacing turns out to be less than the cyclotron frequency, which matches the majority of observed ZP events. In the case of the opposite inequality, the frequency spacing can be comparable with or exceed the cyclotron frequency. It is important that the DPR regions themselves turn out to be very narrow, so the frequency band of the radiating stripes is less than the frequency spacing. This provides the existence of the resolved stripes of enhanced intensity in the dynamic spectrum (Zheleznyakov and Zlotnik, 1975).

Besides, the DPR instability has a rather low threshold over the nonthermal electron number density, which is necessary to overcome the plasma wave damping due to collisions. This explains the pretty frequent appearance of the ZP in the dynamic spectra. An essential part of the plasma mechanism responsible for the origin of solar radio bursts is non-linear transformation of the plasma waves incapable to escape from the corona into electromagnetic radiation easily leaving the source (Zheleznyakov, 2000). There is reason to believe (Zlotnik *et al.*, 2014) that the process of induced scattering by ions or low frequency oscillations is more preferable for the ZP interpretation than the coalescence of two plasma waves. In this case the transformation of plasma waves occurs without significant frequency change, that is, the striped shape of the spectrum persists.

Special attention should be paid to the frequency drift of zebra stripes. Evidently, the change of the zebra stripe frequency is determined by the relative change in the magnetic field and electron number density and significantly depends on the ratio of typical sizes of the height inhomogeneity of the electron number density  $L_N = f_p (df_p/dh)^{-1}$  and the magnetic field  $L_B = f_B (df_B/dh)^{-1}$  (Figure 2). Assume that in the source where  $L_N > L_B$  (Figure 2a) the electron number density remains constant but the magnetic field decreases with time (it is quite natural for the post-flare stage). Then the system of lines describing the harmonics of the cyclotron density is moving down in Figure 2a, and the points of intersections of the system of cyclotron harmonics with the line describing the height dependence of the electron number density, are moving towards the higher frequencies. Since these points of intersection are the frequencies of the zebra stripes, the decrease in the magnetic field results in the positive frequency drift, that is, the frequencies of the zebra pattern increase when the magnetic field decreases in the source with  $L_N > L_B$ . On the contrary, in the source with faster change in the electron number density over the height, when  $L_N < L_B$  (Figure 2b), the frequency drift is negative if the magnetic field decreases. The ZP frequencies can change also in the case, where the magnetic field remains constant, but the electron number density increases or decreases (the dash-and-dash line is moving up and down in Figure 2). Independently of the ratio  $L_N$  and  $L_B$ , the frequency drift is positive if the electron number density increases with time and negative otherwise.

The above model of the ZP source successfully explains the majority of details of the observed solar ZP in the meter and decimeter wave band, in particular, the great number of stripes, the dependence of frequency spacing between the stripes on the frequency, frequency drift, relatively frequent appearance of ZP in the solar radio emission, high polarization of radiation in zebra stripes corresponding to the ordinary mode, and occasional oscillations of the frequency drift velocity. The crucial argument in favor of the ZP theory based on the DPR effect is given by Chen *et al.*, 2011 who proved that the different zebra stripes emerge in the spatially separated sources.

### 3. Interpretation of the "fingerprint" fine structure

As was mentioned above, the "fingerprint" fine structure discussed in the present paper does not look like a typical ZP slowly drifting in time and consisting of a great number (sometimes tens) of stripes of enhanced intensity at a given time.

Nonetheless, let us assume that the bright stripes in Figure 1 emerge in the DPR regions, which correspond to separate harmonics of the cyclotron frequency. Such harmonics have the form of the circular arcs shown by dotted lines in Figure 1. Here in the central part of the event at about 8:32:00, when the frequencies of the zebra stripes reach their minima, the spectrum resembles the usual ZP: the stripes are quasi-horizontal and have a small positive frequency drift before and after the arc center. However, in the course of time the zebra stripe frequencies begin to increase sharply (fast positive drift arises, and its velocity grows with the time), and simultaneously there appears a low frequency branch of the stripe with the negative frequency drift where velocity also grows with the time. At first glance, these two branches are not related to each other, but later they join at the point with infinite velocity of the frequency drift. This means that they cannot be independent. The form of the zebra stripes before the symmetry center of the arc is a mirror image of the form of ZP stripes after the center (see the dotted line in Figure 1): enhanced radiation arises at some frequency which is the start of low and high frequency branches with the positive and negative frequency drift, respectively.

Thus, an essential feature of the dynamic spectrum shown in Figure 1, is the fast frequency drift of the zebra stripes and reversal of the frequency drift direction within the limits of the same harmonic. At each harmonic, there are two frequencies of advanced radiation at a given time. First, we consider in detail a fragment of the spectrum after the symmetry center of the arc selected by a rectangle in Figure 1. Here the advanced radiation appears first at frequencies well separated from each other, then these frequencies become closer, and at the point with infinite velocity of the frequency drift they join and disappear. The model of the source should explain the different signs of the frequency drift: at low frequencies it is positive, but then it changes to negative via an infinite drift velocity. Besides, at a given time no more than two harmonics are observed. It is rather difficult to explain such a behavior of the zebra stripes in the framework of the models shown in Figure 2.

### 3.1. Qualitative interpretation

Let us suppose, however, that the electron number density changes with height in such a way, that its gradient changes in wide limits from rather large values in the upper layers till smaller values in the lower layers. The assumed qualitative dependence of the plasma frequency on height (coinciding with the electron number density in the source) is given in Figure 3 (dash-and-dash line). Let us construct the model of the source in a way similar to that in Figure 2. Assume, that at some time the radiating harmonics (let it be three harmonics with the numbers  $s-1$ ,  $s$ , and  $s+1$ ) intersect the plasma frequency distribution only in the lower-frequency part (Figure 3a). Then three points will appear in the corresponding dynamic spectrum (Figure 3d). When the magnetic field decreases, that is, three lines displaying harmonics are moving down in Figure 3a, the DPR points are moving to the higher frequencies, and so here the usual ZP spectrum is formed with the weak positive frequency drift (as follows from Figure 3a, here  $L_N > L_B$ ). When the magnetic field proceeds to decrease and the DPR points shift to even higher frequencies, the gradient of the electron number density increases, and so does the velocity of the frequency drift (Figure 3d). The most important attribute of the model is that with the further decrease in the magnetic field and motion of the harmonics downwards they start to intersect the line  $f_p(h)$  at two points; see in this connection the moment  $t_2$  (Figure 3b).

Thus, there are always two points determining the zebra stripe within the limits of the same harmonic. Besides, in the high frequency part of the zebra stripe the ratio of the gradients is opposite to that in the low-frequency part, that is,  $L_N < L_B$ . This means that here the DPR frequencies decrease with the further decrease in the magnetic field, which provides the negative frequency drift. Therefore, in the dynamic spectrum the two branches of the harmonics become closer to each other (Figure 3e). Evidently, with the further decrease in the magnetic field (Figure 3c, moment  $t_3$ ) the frequency distance between the DPR points further decreases, the DPR points become closer to each other, and then this harmonic leaves the region of intersection with the line  $f_p(h)$ , i.e. does not have DPR points and disappears from the dynamic spectrum (Figure 3f).

At the moment of touching the curves  $f_p(h)$  and  $sf_B(h)$  the velocity of the frequency drift is infinite. It is just the behavior of the zebra stripes in the observed spectrum at the time after the center of the arc. The apparent almost vertical drift of the zebra stripes is due to rather close values of the gradients of the magnetic field and electron number density.

Similarly, one can interpret the ZP behavior before the center of the arc: the magnetic field increases with the time, the harmonics are moving upwards, and the event develops according to Figure 3 in the direction from c) to a) and from f) to d). The start of the event is presumably determined by the moment at which the velocity distribution function of the non-equilibrium electrons, which is necessary for the DPR effect, is formed. The value of the magnetic field at this time determines, according to the scheme shown in Figure 3, the largest number of the harmonic participating in the event.

Thus, the arc- or loop-like ZP structure in the fingerprint event can be explained by the gradual increase and decrease in the magnetic field in the source

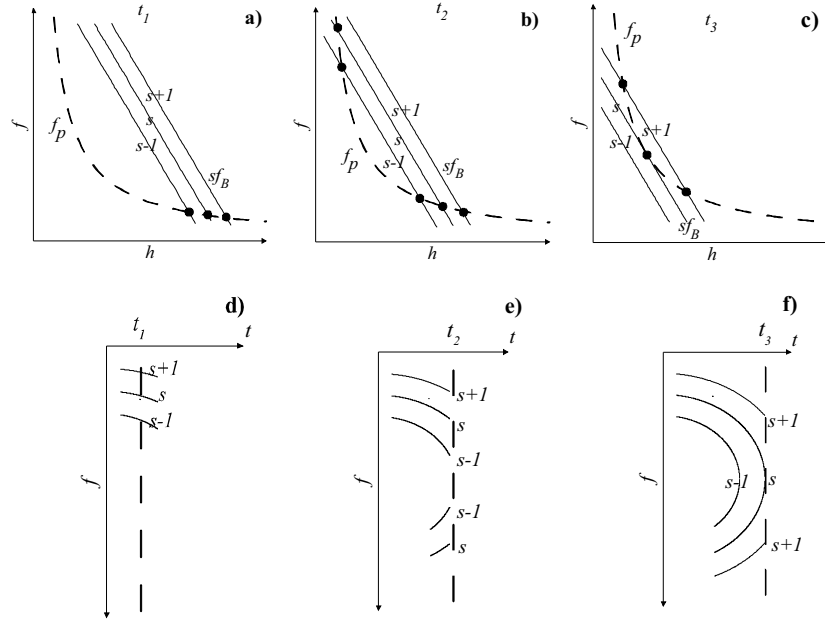


**Figure 3.** Qualitative clarification of the origin of the fingerprint structure as a set of quasi-vertical arcs. The top panel is the source model: dependence of the electron plasma frequency and the frequencies of the electron cyclotron harmonics on the coordinate along the source at three times  $t_1 < t_2 < t_3$ ; the electron number density remains constant, and the magnetic field decreases in time; black circles denote the DPR levels. The lower panel gives the dynamic spectrum with the zebra stripes corresponding to the times  $t_1, t_2, t_3$ .

with electrons that are non-equilibrium over transverse (relative to the magnetic field) velocities, under the condition that the harmonic with a given number has two DPR points at the different heights. Herewith, the numbers of harmonics increase from the "inner" to the "outer" arcs.

The scheme given above illustrates the idea how one can explain the observed details of the fine structure in the form of quasi-vertical arcs basing on the DPR effect. However, in order to explain the fingerprint burst shown in Figure 1 and to be sure that such a scheme can be realized under the coronal conditions, it is necessary to propose the source model which can provide the observed numerical values of the zebra stripe frequencies and the velocities of frequency drift under the real conditions of the solar corona.

### 3.2. Real model of the source of the fingerprint burst

Figure 4 shows the scaled-up numerical record of the dynamic spectrum fragment shown by a rectangle in Figure 1, where the structure with the resolved stripes is seen most clearly. The lines correspond to the peak intensity observed in the zebra stripes. It is the fragment for which we will match the quantitative model of the source. Our purpose is to find such a dependence of the magnetic field and the electron number density on height and such change of these parameters with the time, which provide the location of the DPR levels at the frequencies

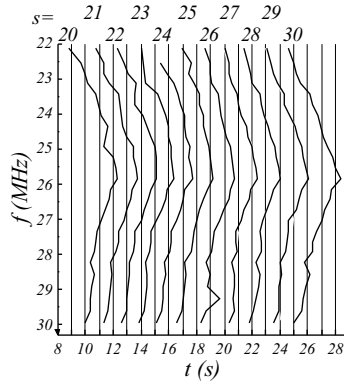


**Figure 4.** Numerical record of the dynamic spectrum fragment selected by the rectangle in Figure 1. The up numerals indicate the numbers of the harmonics of the electron cyclotron frequency accepted in the proposed source model.

corresponding to the observed frequencies of the zebra stripes at each time moment, as well as the successive appearance of the 11 observed harmonics with the time. We will consider distributions at intervals of 1 second and achieve the coincidence of calculated frequencies at the DPR levels with the observed frequencies which are designated in Figure 4 by the points of intersection of observed zebra stripes with the vertical straight lines counted in seconds. The highlighted fragment of the burst takes the time interval 08 : 32 : 09–08 : 32 : 28. Hereinafter the time will be designated only in seconds, for example, the time  $t = 08 : 32 : 13$  will be denoted  $t = 13$ .

As before, for simplicity we consider the magnetic flux tube containing non-equilibrium electrons, i.e. the ZP source, to be located vertically in the corona, that is, we will regard the sources which are non-uniform only over height. Under the real coronal conditions the distribution of the electron number density over height in the decameter radiation sources is well described by the Newkirk model of the coronal ray (Newkirk, 1961):

$$N = 4.2 \cdot 10^4 \cdot 10^{4.32R_S/R}, \quad (3)$$

where  $R_S = 7 \cdot 10^{10}$  cm is the solar radius,  $R$  is the distance from the Sun's center, and  $N$  is expressed in  $\text{cm}^{-3}$ . According to (3), the plasma with electron number density  $6 \cdot 10^6 \text{cm}^{-3} < N < 1.1 \cdot 10^7 \text{cm}^{-3}$ , corresponding to the observed frequency band  $22 \text{MHz} < f \approx f_p < 30 \text{MHz}$ , is located at heights  $5.4 \cdot 10^{10} \text{cm} < h < 7.0 \cdot 10^{10} \text{cm}$ . Correspondingly, the plasma frequency changes with the height as

$$f_p = 1.84 \cdot 10^{2.16/(1+h/7)}, \quad (4)$$

where the height  $h$  and the plasma frequency  $f_p(h)$  are expressed in units of  $10^{10}$  cm and MHz, respectively. The dependence  $f_p(h)$  (4) is shown by dash-and-dot line in Figure 5. In our model, according to Figure 3, a more rapid change in the electron number density gradient with the height is required. The

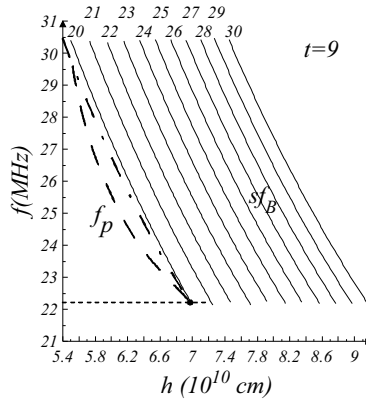


**Figure 5.** Distribution of the electron plasma frequency (dot-and-dash line is the Newkirk model, dash-and-dash line is the deviation from the Newkirk model accepted in the proposed model) and the harmonics of the electron cyclotron frequency (solid lines)  $s = 20 - 30$  over height at the initial time. Here and elsewhere the numerals denote the harmonic numbers accepted in the model. The horizontal dotted line corresponds to the ZP frequency  $f = 22.2$  MHz, observed at  $t = 9$ .

distorted distribution  $f_p(h)$  proposed for the source model, is described by the dash-and-dash line in Figure 5 (below it will be shown how this distribution was obtained basing on observation data).

The height distribution of the magnetic field and, respectively, the cyclotron harmonics is chosen from the following considerations. Firstly, the magnetic field gradient must be rather close to the electron number density gradient, since at each time no more than 1-3 harmonics are observed. It is seen in Figure 2 that if the gradients differ considerably, then the number of harmonics must be much greater. Secondly, in accordance with the concept proposed in Figure 3, the magnetic field gradient must be more and less than the electron number density at the low and high frequency wings of our band, respectively. A system of solid lines displaying such a behavior of the magnetic field at the initial time  $t = 08 : 32 : 09$  denoted below as  $t = 9$  is shown in Figure 5. Note, that without additional information on the magnetic field it is impossible to find in advance the numbers of the harmonics participating in the event. First we consider the smallest harmonic number  $s = 20$ , i.e. choose the set of harmonics  $s = 20 - 30$ , and create the corresponding model of the magnetic field. Then we discuss alternative variants. Thus, in Figure 4 the zebra stripes correspond to the harmonic numbers  $s = 20 - 30$ , counted from the left to the right. For the chosen initial number  $s = 20$  the magnetic field and the cyclotron frequency dependence on height is approximated by the laws

$$B = 2.62 / (1 + h/7.95)^3, \quad f_B = 7.36 / (1 + h/7.95)^3, \quad (5)$$

where  $B$ ,  $f_B$  and  $h$  are expressed in G, MHz and  $10^{10}$  cm, respectively. Note that the specific dependence of the magnetic field on the height does not matter much. It is necessary only for the behavior of the function  $sf_B(h)$  to be described by the curves close to those shown in Figure 5. The distributions given in Figure 5

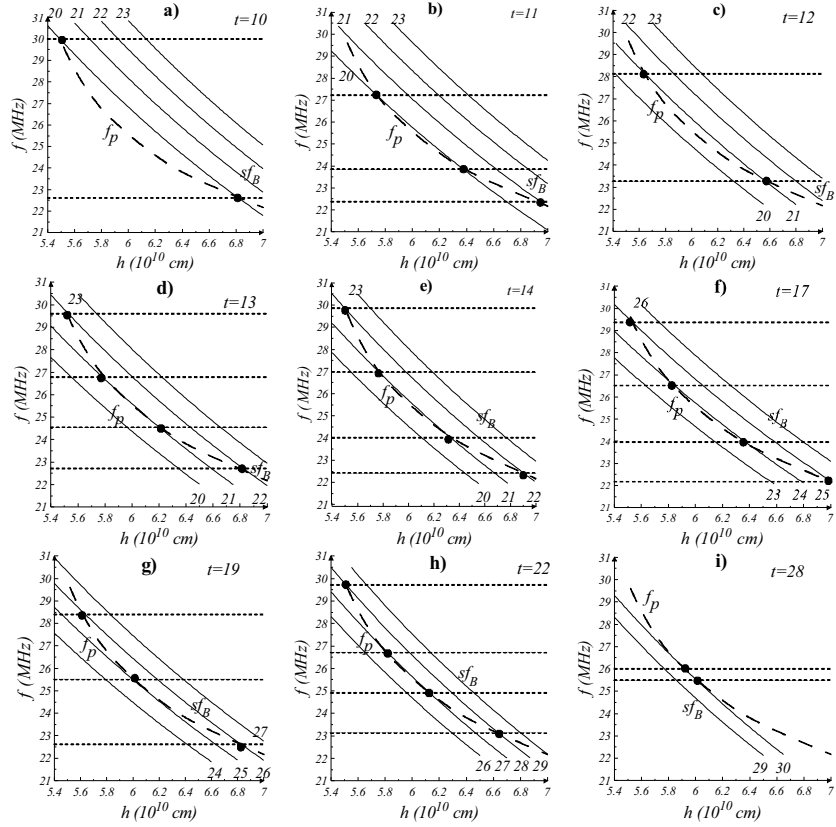


**Figure 6.** The model of the source based on the anomaly of the electron number density constant in time, and the magnetic field decreasing in time: dependence of the plasma frequency  $f_p(h)$  (dash-and-dash line) and the frequencies of the cyclotron harmonics  $s f_B(h)$  (solid lines) at different times (indicated in seconds in the right upper corner of each panel). Here and everywhere the dotted horizontal lines denote the observed frequencies of the zebra stripes at appropriate times. The model fits observations if the points of intersection of the lines  $f_p(h)$  and  $s f_B(h)$ , i.e. the DPR points, denoted by black circles are located on the horizontal lines.

belong to the first moment of the dynamic spectrum under review, when the only zebra stripe is recorded at the frequency  $f = 22.2$  MHz (Figure 4). This frequency is denoted by a horizontal dotted line, which intersects the lines  $f_p(h)$  and  $20 f_B(h)$  at the same point, that is, DPR point. All higher harmonics  $s = 21 - 30$  do not intersect the curve  $f_p(h)$  in our frequency band and therefore cannot be seen in the spectrum. Further we assume that the electron number density remains constant in time, and decrease the magnetic field in such a way that at the subsequent second intervals the points of intersection of the lines  $f_p(h)$  and  $s f_B(h)$ , that is, DPR points, coincide with the observed ZP frequencies.

In succeeding Figures 6a-6i the horizontal dotted lines denote the observed frequencies of the zebra stripes at the times  $t = 10 - 14, 17, 19, 22, 28$  (according to Figure 4). The dash-and-dash line describes the adopted dependence of the

plasma frequency  $f_p$  on the height, and the solid lines present the behavior of the cyclotron frequency harmonics  $sf_B$  as a function of the height  $h$ . The numerals indicate the harmonic numbers. The points of intersection of the curves  $f_p(h)$  and  $sf_B(h)$ , i.e. DPR points, are denoted by black circles. If they coincide with the observed ZP frequencies located at the horizontal dotted lines, then the model fits the observations.

Thus, at the initial moment the only DPR point exists (Figure 5). Let us turn to Figure 6a describing the source in one second, i.e. at  $t = 10$ . The decrease in the magnetic field versus the moment  $t = 9$  is chosen such that the frequency of the zebra stripe  $s = 20$  shifts from the value  $f = 22.2$  MHz in Figure 5 to the frequency  $f = 22.9$  MHz, according to observations (Figure 4). Such decrease is 3%. Surprisingly, it was found that the second DPR point automatically coincides with the observed frequency  $f = 30$  MHz at the high-frequency wing of the zebra stripe  $s = 20$ . When the magnetic field decreases by another 3%, the DPR points at the harmonic  $s = 20$  are close to each other and shift toward the frequencies which are the observed ZP frequencies at the next moment  $t = 11$  (Figure 6b). Moreover, such a decrease in the magnetic field results in that the point of intersection of the harmonic  $s = 21$  with the line  $f_p(h)$  arises just at the frequency where the next zebra stripe is observed. It is important that the change in the magnetic field is selected such that one of the DPR point, i.e. the point of intersection of the lines  $f_p(h)$  and  $sf_B(h)$ , is located on the horizontal line corresponding to the observed ZP frequency at the next moment. Wherein, there is no reason for the rest DPR points to coincide with the observed frequencies of the zebra stripes at the "right" harmonics. Three curves,  $f_p(h)$ ,  $sf_B(h)$  and the observed frequency (horizontal line), cannot intersect at the same point by chance. The fact that such coincidence happens automatically proves that the selected height dependence of the magnetic field and electron number density correctly describes the real behavior of the parameters in the source. It is well confirmed by the further decrease in the magnetic field. The transition to the next second  $t = 12$  (Figure 6c) and decrease in the magnetic field by another 3% is accompanied by increasing convergence of the DPR points at the harmonic  $s = 20$ , in full accordance with the observations, and the emergence of the second DPR point at the high-frequency wing of the harmonic  $s = 21$ . Touching of the curves  $f_p(h)$  and  $20f_B(h)$  corresponds to the point with infinite drift velocity on the dynamic spectrum (Figures 3-4), where the sign of the frequency drift reverses.

The next decrease in the magnetic field by approximately 3% in the transition to the next time moment  $t = 13$  (Figure 6d) results in that the harmonic  $s = 20$  disappears in the dynamic spectrum, the DPR points close up at the harmonic  $s = 21$  and two DPR points arise at the harmonic  $s = 22$ . All newly arising DPR points again coincide with the frequencies of the observed zebra stripes. It should be noted that it is just the moment  $t = 13$  at which there are four DPR points covering the entire frequency band of the event, was selected in order to construct the dependence  $f_p(h)$ . We plotted the height dependence of the frequencies of the cyclotron harmonics with the numbers  $s = 21$  and  $s = 22$ , which, according to observations, are present in the spectrum at this time, then we plotted the horizontal lines corresponding to the observed ZP frequencies and

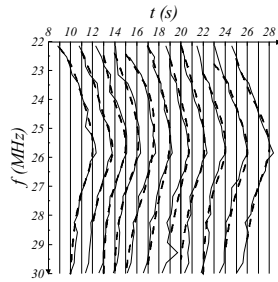


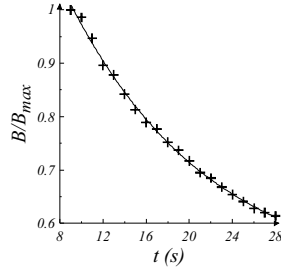
**Figure 7.** Comparison of the observed spectrum (solid lines) with calculated smoothed spectrum (dash-and-dash lines) in the source model given in Figures 5-6.

drew the curve  $f_p(h)$  through 4 points using spline interpolation. Further, all the previous and subsequent time moments were counted for this electron number density distribution over height. It should be emphasized once more that there is no reason to believe that the DPR frequencies must coincide with the observed frequencies of the zebra stripes when the magnetic field changes. Changing the velocity of the magnetic field decrease we can adapt only one point, but in no way it can happen by chance that at other frequencies the three curves (dependences  $f_p(h)$ ,  $sf_B(h)$  and the horizontal lines denoting the observed frequency of the zebra stripe) intersect at the same point. Figure 6e describing the source model at the moment  $t = 14$ , where the harmonic  $s = 21$  exits from resonance, and moreover, all three mentioned curves intersect at the same points, confirms once more the fidelity of the suggested model.

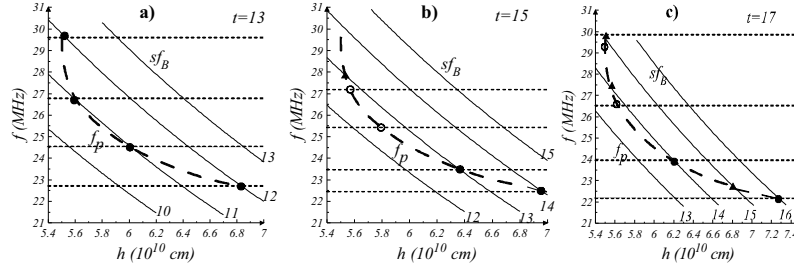
Further, we successively decrease the magnetic field by approximately 3% per second and every time get the coincidence of the model values of the DPR frequencies with the observed ZP frequencies. At the end of the event, the rate of the magnetic field decrease that is necessary to "catch" the observed frequencies, must be reduced to 1.5%. For illustration, we give the source models at the moments  $t = 17, 19, 22, 28$  (Figures 6f, 6g, 6h, and 6i, respectively). The coincidence of the model and observed frequencies is beyond doubt.

Figure 7 gives the resulting dynamic spectrum for all harmonics in the time interval  $t = 9 - 28$ . The solid and dotted lines represent the observed and calculated (smoothed) spectra, respectively. Evidently, the suggested source model with decreasing magnetic field explains quite well the observed details of the fingerprint burst in a separated fragment of the event.

As was said above, in order to explain the observed frequency drift in the selected fragment of the fingerprint burst the magnetic field should decrease by approximately 3% at the beginning and by 1.5% at the end of the event. Figure 8 shows the relative change in the magnetic field during the entire selected fragment of the event. Evidently, the total change must be rather significant, by approximately 40% for 18 seconds. The values of the magnetic field in the source obtained under the assumption that the observed harmonics have the numbers  $s = 20 - 30$ , amount to  $B \approx (0.3 - 0.5)$  G, which is quite usual for the decameter burst sources emerging from heights of the order of several hundred thousands of kilometers above the photosphere.



**Figure 8.** Relative decrease in the magnetic field with time which is necessary to fit the observed spectrum in the source model given in Figures 5-6.



**Figure 9.** The same as in Figure 6 for the harmonic set  $s = 10 - 20$  at three times indicated in seconds in the right upper corner of each panel. Here and everywhere the black circles denote the DPR points coinciding with the observed ZP frequencies, white circles denote the points of intersection of the line  $f_p(h)$  with the observed frequencies which are not DPR points, and triangles denote the DPR points not coinciding with the observed ZP frequencies.

### 3.3. Alternative models of the fingerprint burst

First of all, we discuss the harmonic numbers selected in the source model for the quantitative explanation of the fingerprint spectrum. Calculations show that using the smaller harmonic numbers to interpret the fragment selected in Figure 1 seems to be rather embarrassing. This follows from Figure 9, where the attempt to fit the observations using harmonics  $s = 10 - 20$  is shown. Similar to the set of harmonics  $s = 20 - 30$ , we selected the close height gradients of the plasma frequency and the 10th harmonic of the cyclotron frequency. Then, using the four observed ZP frequencies at the moment  $t = 13$ , we plotted the possible deviation of the plasma frequency height distribution from the Newkirk model (Figure 9a). It turned out that in order to achieve the coincidence of the DPR points with the observed frequencies in the subsequent times, the magnetic field must decrease more quickly than in the above model (by 6-7% per second), which results in more significant change in the magnetic field during all the burst. What is more important, no attempts to get the coincidence by the 4 points in the subsequent times by decreasing the magnetic field give the desired results. Figures 9b-9c show the magnetic field distributions over height at the times  $t = 15$  and  $t = 17$  obtained for the magnetic field decrease which gives the best fit for the observed ZP frequencies at those times in Figure 4 (under the condition that the set of harmonics, i.e. the top row of numbers is changed from

$s = 20 - 30$  to  $s = 10 - 20$ ). Black circles denote the DPR points (that is the points where the model value of the plasma frequency is equal to the frequency of the cyclotron harmonic) coinciding with the observed ZP frequencies, that is, located on the horizontal dotted lines. White circles refer to the frequencies of the observed zebra stripes on the line  $f_p(h)$ , i.e. the points through which the corresponding harmonics "must" pass. In Figure 9b (the moment  $t = 15$ ) the magnetic field is reduced by 13% versus the moment  $t = 13$ , and two DPR points in the low-frequency wing of the spectrum coincide with the observed ZP frequencies. However, in the high-frequency part the model and observed curves move away from each other. According to observations, the curve corresponding to the harmonic  $s = 12$  must touch the curve  $f_p(h)$  at a frequency 25.5 MHz at a point shown by a white circle, but at this frequency the two mentioned curves are well separated. Besides, the very high frequency DPR point denoted by a triangle, also is not located at the observed frequency 27.2 MHz. Figure 9c relating to  $t = 17$  demonstrates still greater divergence of the observed ZP frequencies and the values required by the model. Here, the magnetic field is decreased by 9% versus the moment  $t = 15$  in order to provide the intersection of the curve corresponding to the harmonic  $s = 14$  with the curve  $f_p(h)$  at the horizontal line denoting the observed frequency 24.0 MHz. But all the rest three DPR points are not located at the horizontal lines, that is, differ markedly from the observed ones. At more late times this effect is impaired, and no changes in, for example, the magnetic field gradient can increase such a coincidence of the observed and calculated ZP frequencies, as in Figure 6 for the set of harmonics  $s = 20 - 30$ . The reason is that the harmonics with relatively low numbers are too spaced, while in the set  $s = 20 - 30$  the distance between the harmonics much better fits the observational ZP frequency spacing.

A similar attempt to create the model with the harmonic set  $s = 30 - 40$  also failed. In this case, the harmonics turned out to be located too close to the neighboring ones, and the coincidence of the observed and calculated values cannot be reached. Besides, it should be noted that the high numbers of harmonics can result in breaking the conditions of electron trapping in a magnetic trap since the plasma parameter

$$\beta = 8\pi\kappa TN/B^2 = 2 (f_p^2/f_B^2) (v_T^2/c^2), \quad (6)$$

describing the ratio between the gas-kinetic pressure and magnetic pressure becomes not negligibly small.

It is worth noting, however, that the obtained result (that the numbers of harmonics in the interval from 20 to 30 fit the spectrum in the selected fragment best of all) cannot be regarded as a way of accurate measurement of the magnetic field in the ZP source. Firstly, it is clear that the model can be adapted for the sets of harmonics, say,  $s = 18 - 28$  or  $s = 23 - 33$ . Secondly, the above model implies only a primitive way of simply decreasing the magnetic field, which is the same at all heights. At the same time, the magnetic field distribution over the source can change in a more complicated way, for example, by variation of the gradient. Thus, the values of the magnetic field obtained from matching of observed ZP frequencies and the cyclotron frequency harmonics (see the text

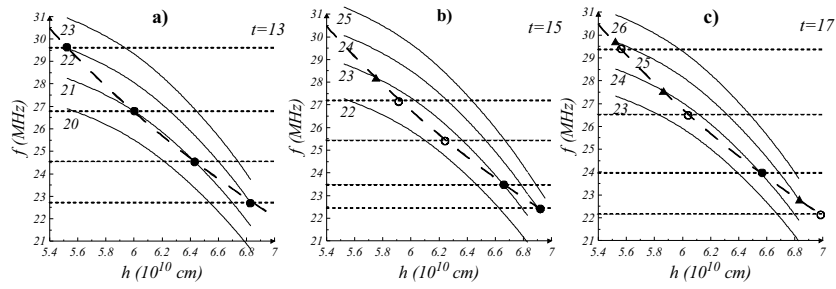


**Figure 10.** The source model based on the anomaly of the magnetic height distribution decreasing in time and Newkirk distribution of the electron number density constant in time: dependence of the plasma frequency  $f_p(h)$  (dash-and-dash line) and the frequencies of the cyclotron harmonics  $sf_B(h)$  (solid lines) on height at three times indicated in seconds in the right upper corner of each panel.

below) can be considered only as approximate ones. However, the example given above for the harmonic set  $s = 10 - 20$  shows that the model does not permit arbitrary choice of the harmonic numbers.

All said above, including the determination of the harmonic numbers  $s = 20 - 30$ , relates only to the selected fragment for numerical analysis in the dynamic spectrum in the time interval 08:32:09-08:32:28 in Figure 1. However at the time before that fragment one can also distinguish quasi-vertical arcs as sebra stripes. Analysis shows that the spectrum after the center of the event contains the harmonics with numbers down to  $s = 5$ . This fact also favors the correctness of selected harmonic numbers.

The peculiarities of the fingerprint spectrum can be formed in the source with somewhat different height distributions of the magnetic field and electron number density. The example of such distributions is given in Figure 10. In this case, the electron number density has no peculiar properties and corresponds to the Newkirk distribution, and the magnetic field has a deviation in the form of "convexity" at some height interval. It is easy to see that in this case the dynamic spectrum as a set of quasi-vertical arcs with the opposite directions of the frequency drift in the high- and low-frequency wings can also be formed. The decrease in the magnetic field, i.e. moving of the "convexity" downwards in Figures 10a-10c and intersection of the curve  $f_p(h)$  with higher and higher harmonics results in that the DPR points become closer to each other and later disappear from the resonance. Thus, the main properties of the fingerprint spectrum can be qualitatively explained in such a model.

Following the technique described above for constructing the distribution distortion, i.e. plotting the height change of the magnetic field via four observed ZP frequencies at a given time, one can find the rate of the magnetic field decrease which results in coincidence of the model DPR points with the observed ZP frequencies at subsequent times. However, the analysis shows that if only the value of the magnetic field decreases, i.e. the anomaly constructed for one time moment is simply moving downwards, it is impossible to provide fitting the observations. It is seen in Figures 10b-10c that the magnetic field distribution

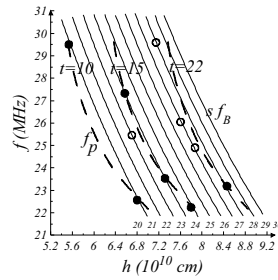


**Figure 11.** The source model based on the anomaly of the electron number density height distribution moving up in the corona, and a time-constant magnetic field: dependence of the electron plasma frequency  $f_p(h)$  (dash-and-dash line) and the frequencies of the cyclotron harmonics  $s f_B(h)$  (solid lines) on height at three times indicated in seconds.

fitting observations at  $t = 13$  gives a strong difference between calculated DPR points and the observed ZP frequencies at subsequent times (DPR points denoted by triangles are far away from the measured ZP frequencies denoted by white circles). With the further decrease in the magnetic field the discrepancy of the observed and calculated values becomes still more significant. Thus, in this case the attempt to adapt the quantitative model fitting the observations fails.

Further we study the possible source models with a time-constant magnetic field and changing electron number density. It is seen from the qualitative analysis shown in Figure 2 that the change in the electron number density in time, as well as the magnetic field, can explain the frequency drift of the zebra stripes and, therefore, the observed peculiarities of the fingerprint spectrum.

First we consider the electron number density distribution shown in Figure 5 and assume that the plasma frequency increases in time (the dash-and-dash line in Figure 5 is moving upwards), and the magnetic field remains constant. Evidently, the main property of the fingerprint spectrum, namely, the presence of two DPR points at a given harmonic, their closing with time and the further disappearance, is quite explainable under this assumption. However, all the spectrum cannot be obtained in such model: as time proceeds, the increasing electron number density outputs the plasma frequency and DPR points from the observed frequency band.

There is another option. Let the electron number density distortion as a "convexity" moves upwards in the corona, that is, moves to the right in Figure 11. Here the main properties of the fingerprint spectrum also can be explained. The analysis of such a motion shows that a good coincidence of the calculated and observed frequencies is unachievable, although the three times fixed in Figure 11 indicate that the discrepancy is not so significant as for other models. Besides, the model shown in Figure 11 assumes that the anomaly of the electron number density moves as a whole, but in principle, it is quite possible that it changes its shape with time and can provide a better fit with observations. However, this means that such motion of the anomaly of the electron number density distribution in the background corona must be accompanied by synchronous motion of the region where the non-equilibrium electrons are located, which is hard to realize. Furthermore, in our model, as follows from Figure 11, the

source must run the distance  $1.7 \cdot 10^{10}$  cm for 12 seconds, which corresponds to a high velocity of  $1.5 \cdot 10^9$  cm/s. This exceeds by two orders of magnitude the sound velocity at an appropriate temperature and the electron number density ( $v_s \sim 10^7$  cm/s). But it is the sound velocity which can be expected for any density perturbation propagating in the coronal plasma.

Therefore, the deviation of the electron number density distribution from the usual height dependence and its change in time can hardly explain the observed peculiarities, and the said variant looks less preferable as a reason to form the fingerprint spectrum compared to the model with changing magnetic field shown in Figure 6.

#### 4. Discussion and Conclusions

Thus, the fine structure of the solar decameter radiation as a fingerprint spectrum is explained in the framework of the DPR mechanism in the solar coronal trap with the specific height distribution of the electron number density and a relatively fast change in the magnetic field with time. The main properties of the fingerprint spectrum, namely, the fast frequency drift of the zebra stripes, the presence of two frequencies of advance brightness in a given harmonic at a given time, and the opposite direction of the frequency drift at these frequencies, automatically follow from the model. The proposed model is realized with reasonable parameters determining the physical conditions in the trap (with a slight deviation of the height distribution of the electron number density from the typical Newkirk model): the source is located at the height  $h \sim (5-7) \cdot 10^{10}$  cm above the photosphere, the electron number density varies within  $N \sim (0.6-1.1) \cdot 10^7$  cm<sup>-3</sup>, and the magnetic field is  $B \sim (0.3-0.5)$  G.

The estimations given above refer only to the selected fragment shown by a rectangle in Figure 1 for quantitative analysis. If the whole burst fingerprint is considered, then judging by the low frequency boundary of the spectrum  $f = 15$  MHz, we can estimate that the source extends up to the heights of the order of  $h \sim 10^{11}$  cm, and the low boundary of the electron number density is  $\sim 3 \cdot 10^6$  cm<sup>-3</sup>. The said height interval is determined by the boundaries of the trap where the electrons non-equilibrium over transverse velocities relative to the magnetic field are present. The life time of the burst is also determined by the life time of the non-equilibrium electrons in the trap. According to the present interpretation, the electrons are injected into the trap (with specific distribution of the electron number density over height) at approximately 08:31:20. At this time, the magnetic field is weak enough, so the DPR is realized only for the harmonics with the number about  $s \approx 30$ . Then the magnetic field begins to increase, the DPR points in the low and high frequency wings of the zebra stripe shift toward the higher and lower frequencies, respectively, and also the harmonics with smaller numbers enter the resonance region. Then the magnetic field reaches its maximum at about 08:32:00 where the zebra stripes are quasi-horizontal, which corresponds to Figure 3a. Thereafter the magnetic field begins to decrease, resulting in appearance of fast drifting zebra stripes with the opposite "convexity" on the dynamic spectrum (Figures 3b-3c). The end of the burst

at 08:32:28 is associated with the disappearance of the non-equilibrium electrons from the source.

It should be noted that the change in the magnetic field occurs simultaneously over the entire height of the source, that is in the interval  $h \sim (5 - 10) \cdot 10^{10}$  cm corresponding to the observed frequency band  $f \sim (20 - 30)$  MHz. It is not excluded that the source extends to the lower heights than the above value: the low frequency boundary is clearly seen in the spectrum, while the high frequency one may be cut off by the boundary of the available frequency band of observations. Simultaneous change in the magnetic field over the entire height of the source proves that the observed zebra stripes as quasi-vertical arcs cannot be associated with any perturbation propagating along the loop in the corona, but are due, most probably, to some self-consistent process embracing the whole loop. The best candidate for such a process is non-linear fast magneto-acoustic (FMA) oscillation of the magnetic flux tube, which is accompanied by compression and depression of the non-uniform (over height) magnetic field. Such an idea is confirmed by the numerical estimations. The period of the FMA oscillations is determined by the relation (Stepanov *et al.*, 2012):

$$T \approx \frac{2.5r}{V_A}, \quad (7)$$

where  $r$  is the radius of the magnetic flux tube cross-section and  $V_A$  is the Alfvén velocity

$$V_A = \frac{B}{\sqrt{4\pi m_i N}} = c \frac{f_B}{f_p} \sqrt{\frac{m}{m_i}}. \quad (8)$$

( $m_i$  is the ion mass). Since the Alfvén velocity depends only on the ratio  $f_B/f_p$ , in the DPR regions where  $f_B/f_p = 1/s$ , it remains constant and depends only on the harmonic number  $s$ :

$$V_A = \frac{c}{s} \sqrt{\frac{m}{m_i}}. \quad (9)$$

For the selected set of harmonics  $s = 20 - 30$  the Alfvén velocity takes quite reasonable for the corona values  $v_A \approx (2.3 - 3.5)10^7$  cm/s. Evidently, the Alfvén velocity changes with the height and decreases when moving to the regions where the harmonics with the larger numbers are generated. Thus, if the dependence of the tube radius  $r$  on height is neglected, then the period of the FMA oscillations turns out to be proportional to the harmonic number  $s$ :

$$T \approx \frac{2.5r}{c} s \sqrt{\frac{m_i}{m}}. \quad (10)$$

Obviously, the life time of the oscillation which is certainly different at different heights, as well as the Alfvén velocity, turns out to be proportional to the harmonic number. It is just the same dependence which is seen in the observed spectrum: the harmonics with larger numbers (the arcs of the larger radii) take a larger time interval than the harmonics with smaller numbers (the arcs of the

smaller radii). For the tube with the usual radius  $r = 5 \cdot 10^8$  cm and selected harmonic set  $s = 20 - 30$ , the oscillation time (10) is

$$T \approx (35 - 55)s, \quad (11)$$

which is fully consistent with the observed life times of the arcs in the dynamic spectrum in Figure 1. The non-linear character of the oscillation easily permits a significant change in the magnetic field magnitude in time, which is necessary to explain the fingerprint spectrum within the framework of the proposed interpretation.

It should be noted that the FMA oscillations contain not only a change in the magnetic field, but also a change in the electron number density. However, the relative change in the electron number density can be neglected for small values of the parameter  $\beta$  (6).

It should also be mentioned that the above estimations are rather approximate. The point is that in the non-linear wave the harmonic number is associated with the total magnetic field  $B = B_0 + \Delta B(t)$ , but the velocity of propagation remains constant:  $V_A = B_0 / \sqrt{4\pi N m_i}$ . If the magnetic field changes significantly, then the life time of oscillations in some harmonics can differ from the values in Eq. (10). Nonetheless, the increase in the life time with the harmonic number predicted by the model persists, and it undoubtedly favors of the proposed interpretation.

Thus, the presented model of the source is able to explain the details of the unusual frequency drift of the stripes of enhanced intensity in the observed fingerprint spectrum within the framework of the DPR mechanism under quite reasonable physical conditions (height distribution of the magnetic field and the electron number density) in the coronal trap. The necessary properties of the source model are, firstly, the closeness of the gradients of the magnetic field and the electron number density (in order to provide a little zebra stripes at a given moment), and, secondly, the opposite relation between these gradients at upper and lower parts of the source (in order to provide different signs of the frequency drift in high and low frequency parts of the spectrum). Of course, the selected harmonic numbers, the proposed deviation of the electron number density distribution for the Newkirk model and the height dependence of the magnetic field could not be found unambiguously by the observed spectral features. However, as is shown above, the proposed model provides quite a good quantitative matching of the observed and predicted by the model parameters of the fingerprint burst, and really gives the reliable estimations of the physical conditions in the source.

**Acknowledgements** This work was partly supported by RFBR Projects Nos.13-02-00157 and 14-02-00133 (E.Ya.Z and V.V.Z.) and FP7 Project SOLSPANET (FP7PEOPLE-2010-IRSES-269299) (V.N.M., A.A.K and V.V.D).

## References

Aurass, H., Klein, K.-L., Zlotnik, E.Ya., and Zaitsev, V.V.: 2003, *Astron. Astrophys.* **410**, 1001.

- 
- Braude, S.Y., Megn, A.V., Ryabov, B.P., Sharykin, N.K., Zhouck, I.N.: 1978 *Astron. Astrophys. Suppl.* **54**, 3.
- Chen, B., Bastian T.S., Gary D.E., Jing, J.: 2011, *Astrophys. J.* **736**, 64.
- Chernov, G.P.: 2006, *Space Sci.Rev.* **127**, 195.
- Kuijpers, J.: 1975, *Astron. Astrophys.* **40**, 405.
- Kuznetsov, A. A., Tsap, Yu. T.: 2007, *Solar Phys.* **241**, 127.
- Melnik V. N., Konovalenko A.A., Abranin E.P., Dorovskyy V.V., Stanislavsky A.A., Rucker H.O., Lecacheux A.: 2005, *Astronom. and Astrophys.Trans.* **24**, 391.
- Melnik V.N., Rucker H.O., Konovalenko A.A., Dorovskyy V.V. Abranin E.P., and Lecacheux A.: 2011, in Rucker H.O., Kurth W.S., Louarn P., and Fischer G. (eds.) *Planetary Radio Emissions VII*, Austrian Academy of Sciences Press, Vienna, 343.
- Melnik V.N., Rucker H.O., Konovalenko A.A., Dorovskyy V.V., Abranin E.P., Brazhenko A.I., Thide B., Stanislavskyy A.A.: 2008, in Pingzhi Wang (ed.) *Solar Physics Research Trends*, Nova Science Publishers, New York, 287.
- Newkirk, G.: 1961, *Astrophys. J.* **131**, 983.
- Stepanov A.V., Zaitsev V.V., Nakariakov V.M.: 2012, *Coronal Seismology*, WILEY-VCH Verlag GmbH&Co.KGaA, Germany, 45.
- Winglee, R. M. and Dulk, G.: 1986 *Astrophys. J.* **307**, 808.
- Zheleznyakov, V.V.: 2000, *Radiation in Astrophysical Plasmas*, Kluwer Academic Publishers, Dordrecht.
- Zheleznyakov, V. V., Zlotnik, E. Ya.: 1975, *Solar Phys.* **43**, 431; **44**, 461.
- Zlotnik, E.Ya.: 2009, *Central European Astrophys. Bull.* **33**, 281.
- Zlotnik, E.Ya., Sher, E.M.: 2009, *Radiophys. Quantum Electronics* **52**, 88.
- Zlotnik, E. Y.; Zaitsev, V. V.; Altyntsev, A. T.: 2014, *Solar Phys.* **289**, 233.